Electrorheological Fluids Based on Metallo-Supramolecular Polyelectrolyte–Silicate Composites

Guntram Schwarz,*[†] Stefan Maisch,[†] Stefan Ullrich,[†] Julian Wagenhöfer,[†] and Dirk G. Kurth[†,‡]

[†]Chemical Technology of Advanced Materials, Julius-Maximilians-University of Würzburg, Röntgenring 11, D-97070 Würzburg, Germany and

[‡]Fraunhofer Institut für Silicatforschung ISC, Neunerplatz 2, D-97082 Würzburg, Germany

Ⓢ Supporting Information

ABSTRACT: We present an innovative concept for the design of electrorheological fluids (ERF) based on a dispersed phase of rigid-rod-shaped metallo-supramolecular polyelectrolytes (MEPE) intercalated in mesoporous SBA-15 silica. While applying an electric field to this composite dispersed in silicone oil, rheological measurements reveal a strong increase in the storage modulus, indicating the solidification of the fluid. Besides the strong electrorheological effect and the low current densities, we note that the required amount of MEPE is five times lower than in comparable host–guest ERFs. Composites based on mononuclear complexes do not show a comparable electrorheological effect.

KEYWORDS: electrorheological fluids, supramolecular chemistry, SBA-15, self-assembly, electrorheology
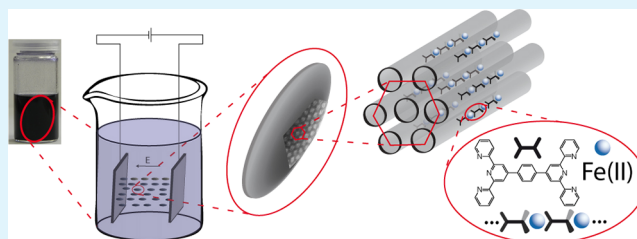
INTRODUCTION

Electrorheological fluids (ERF) are colloidal suspensions whose rheological properties react to an applied electric field.[1] It is generally accepted that the electrorheological (ER) effect is based on the dielectric polarization of particles in an insulating medium. The dispersed phase responds to the electric field by forming fibrous structures (see Figure S1 in the Supporting Information) resulting in the solidification of the fluid within the order of milliseconds.[2] The response is reversible and is controlled by the electric potential and also depends on the size, volume fraction, and permittivity of the particles. These properties make ERFs ideal for a wide range of applications, e.g., as shock absorbers, clutches and haptic devices. Therefore, a broad range of electroactive materials has been studied including polyelectrolytes, biomolecules, or coated nanoparticles showing the so-called giant electrorheological effect.[3] However, applications of ERFs in technical devices are limited either because of high current densities, high basis viscosities, or an insufficient ER-effect.

RESULTS AND DISCUSSION

Metal-ion-induced self-assembly of the rigid ditopic terpyridine ligand 1,4-bis(2,2′:6′,2″-terpyridine-4′-yl)benzene, L1, with iron(II) acetate, Fe(OAc)$_2$, in aqueous solution leads to rodlike metallo-supramolecular coordination polyelectrolytes (MEPE), whereas the ligand 4′-(phenyl)-2,2′:6′,2″-terpyridine, L2, forms mononuclear Fe(L2)$_2$ complexes (MC).[4] The formation of Fe-MEPE and Fe-MC is schematically shown in Figure 1.

Whereas Fe-MC is a discrete molecular species, MEPEs are macromolecular assemblies with length up to several hundred nanometers in solution[4] and can, therefore, be considered as
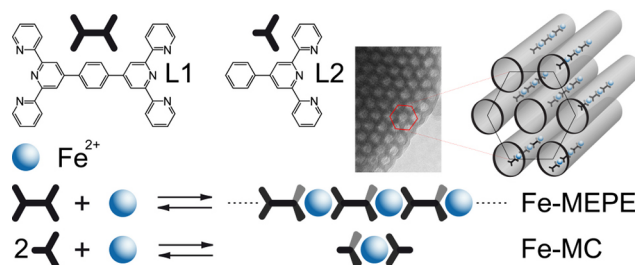

Figure 1. Top left: Metallo-polyelectrolyte (Fe-MEPE) and the mononuclear complex (Fe-MC) are based on Fe(II) as the metal ion and the ligand 1,4-bis(2,2′:6′,2″-terpyridine-4′-yl)benzene, L1, or the ligand 4′-(phenyl)-2,2′:6′,2″-terpyridine, L2, respectively. Bottom: Scheme of the self-assembly process. The pseudo-octahedral coordination geometry is indicated by the wedges; the counterions are not shown. Top right: TEM image of a SBA-15 particle edge revealing the hexagonal orientated mesopores and schematic illustration of MEPE incorporated in the pores.

colloidal systems carrying positive charges. Zetapotential measurements reveal a potential of 52 ± 2 mV at pH 7 and room temperature, indicating a stable colloidal solution. The charge can be utilized to incorporate MEPEs into various architectures such as thin films,[5] liquid crystals or nanostructures.[6] Here, we wish to present the potential of composites of MEPEs intercalated in mesoporous SBA-15 as active materials in electrorheological fluids.

Neat SBA-15 is synthesized according to literature procedure.[7] Surface (REM) and transmission (TEM) electron microscopy show rodlike SBA-15 particles with lengths up to 1000 nm and diameters of 50−200 nm. Small-angle X-ray scattering (SAXS) measurements in the transfer momentum, q, range from 0.3 to 1.6 nm^{-1} show characteristic peaks at q = 0.87, 1.51, and 1.74 nm^{-1} (±0.01) (see Figure S2 in the Supporting Information), corresponding to the lattice planes (100), (110), and (200).[8,9] The SAXS data is in agreement with the above-mentioned TEM measurements (Figure 1). Nitrogen sorption measurements in the relative pressure range of 0.05 to 0.3 reveal a specific surface area of 712 ± 1 m^2 g^{-1} using the Brunner, Emmett, and Teller (BET) multipoint method.

The total pore volume is determined to be $1.28 \times 10^{-06} \pm 0.02 \times 10^{-06}$ m^3 g^{-1}. Using the Kelvin equation, the average diameter of the cylindrical pores is calculated to be D = 7.4 nm. The external particle surface is estimated using the specific surface area and the surface area of the pores to be 17.3 m^2 g^{-1}.

For this study, the ligands L1 and L2 and the corresponding complexes are synthesized according to literature procedures.[4,10] Glacial acetic acid (GAC) or deionized water is used as solvent for the preparation of the composites. Either 858 mg of Fe-MEPE or 951 mg of Fe-MC is dissolved in 1 L of the solvent, equivalent to a concentration of 1.2 mmol L^{-1}. After 1 h of stirring, 2.15 g of SBA-15 is added and the resulting suspension is stirred for 24 h. The solid is separated by vacuum filtration and washed with deionized water until the washing liquid is colorless. The purple-colored solid is suspended again in 1 L water for 60 min, then filtrated and dried under 4 mbar vacuum for 48 h at 60 °C and 2 h at 170 °C. Themogravimetric measurements combined with mass-spectrometry reveal that a temperature of at least 120 °C is needed to evaporate the whole solvent from pure SBA-15 and 150 °C from the composites. The organic components in the composites begin to decompose at 220 °C, so a temperature of 170 °C was set for the second drying period.

The estimated pH of the solution containing Fe-MEPE or Fe-MC is 1.8 for GAC and 5.5 for water, respectively. Zetapotential measurements of pure SBA-15 were carried out in aqueous solution using HCl and NaOH to adjust the pH in a range from pH 1 to 10. At pH 5.5 a zetapotential of −26 ± 4 mV is observed and at pH 1.8 +15 ± 4 mV, respectively. The isoelectric point occurs at pH 2.8. At larger pH values, depronated silanole groups predominate the charge balance at the internal and external particle surface. Under these conditions, the elctrostatic attraction between the negatively charged pore walls of SBA-15 and the positive charged species facilitates intercalation.[8,11] Thus, we assume that in acid at pH 1.8 the loading of positively charged SBA-15 would be unfavorable. The loading is estimated by inductively coupled-plasma mass-spectrometry (ICP-MS) of the dried material measuring the mass of iron in the composite. For 1000 mg of SBA-15, the loading of MEPE in water is 15.6 mg (1.56% w/w), and in GAC 151 mg (15.1%) We note that a loading of 15.1% Fe-MEPE in unsubstituted SBA-15 using the described one step method has not been achieved before, e.g., Akcakayiran et al. reached a maximal loading value of 6% for Fe-MEPE in SBA-15.[11]

The loading of SBA-15 depends on the interactions and the size of the guest molecules. In general, the loaded quantity increases with the ratio of mesopore-diameter to guest molecule size.[12] As mentioned above, in water Fe-MEPE forms rods with lengths up to several 100 nm. Hence, only

species a few nanometers in length can freely diffuse into the pores, while the adsorption of larger rods is severely hindered. Under acidic conditions the chain length of Fe-MEPE decreases thus facilitating loading into the pores (see below). Washing with water will increase the pH value, promoting metal-ion-induced self-assembly and formation of larger rods, which are now being trapped in the pores because of the large size and the increased interactions with the pore wall.

The viscosity of polymers in solution increases with the chain length of the species. Thus, the viscosity of the solvents, η_0, and of 1.2 mmol L^{-1} MC and MEPE solutions, η_C, were measured at 20 °C using Ubbelohde capillary viscosimetry. For MEPE and MC in GAC the specific viscosity $\eta_{sp} = \eta_0/\eta_C$ amounts to 0.94 ± 0.1 and for MC in water 1.01 ± 0.1, respectively, indicating that the compounds do not significantly affect the viscosity of the solvent. In contrast, the aqueous MEPE solution has a specific viscosity of 1.41 ± 0.1. Therefore, we conclude that MEPE in water forms macromolecular assemblies increasing the viscosity, whereas in acid the size of the MEPE rods is considerably shortened.

Although we cannot experimentally determine the amount of MEPE on the outer surface, we can estimate the distribution of MEPE on the inner and external surface of the particles. If MEPE is adsorbed on a surface coated with polystyrolsulfonate (PSS) and washed twice with water for 5 min, UV−vis measurements show that only a single layer of MEPE remains on the surface. It should be noted that PSS offers the same or even a higher surface-charge density than SBA-15.[13,14] We therefore assume that at most a single layer remains on the particle surface. A monolayer of MEPE on the SBA-15 particles with an external surface area of 17.3 m^2 g^{-1} would correspond to 11.3 mg g^{-1} if we consider an area of 1.55×1.2 nm^2 or 1.8×10^{-18} m^2 and a molar mass of 714.56 g mol^{-1} for a single MEPE repeat unit.[6] We conclude that at least more than 90% of MEPE is adsorbed into the pores. Nitrogen sorption measurements of the MEPE-loaded SBA-15 show a reduced pore volume from 1.28×10^{-06} to 0.63×10^{-06} m^3 g^{-1} ($\pm 0.03 \times 10^{-06}$) supporting this conclusion.

The ERFs are prepared by suspending 10 wt % of the dried composites in silicone oil, M10. The notation M10 corresponds to the basis viscosity of 10 mPa s^{-1}. On the basis of the determined MEPE uptake into the pores of SBA-15, the resulting fluids contain either 0.16 or 1.51 wt % MEPE and are named **ERF1** and **ERF2** in the following. **ERF3** corresponds to 0.5 wt % MC. Neat SBA-15 (10 wt %) in silicone oil is used as reference (**REF**).

Through dynamic oscillatory measurements we obtain information about the viscoelastic properties of the ERF. The storage modulus, G', corresponds to the energy stored and released from the elastic structure and the loss modulus, G'', to the dissipated energy into the system, respectively. Without an electric field the samples (**REF**, **ERF1−3**) do not show a distinct linear viscoelastic region. Within strains from 0.001 to 0.2% the samples can be considered as viscoelastic solids or gels based on an average tan $\alpha = G''/G' < 1$. Applying a field, E_f, of ≥1 kV mm^{-1} amplitude sweeps at a constant angular frequency of 10 s^{-1} reveal a linear viscoelastic region within the above-mentioned strains, indicating the formation of a structured liquid for all ERF with higher values for G' and G'', respectively (see Figure S3 in the Supporting Information). The storage moduli, G', of the ERFs and the REF at constant strain of 0.01% as a function of E_f are shown in Figure 2. Raising the field from 0 to 5 kV mm^{-1}, the modulus G' of neat SBA-15
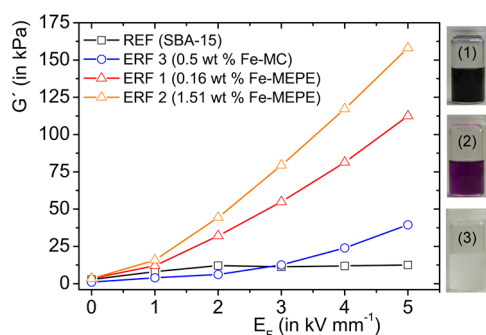
Figure 2. Storage moduli, G', of ERF1 (red triangles), ERF2 (orange triangles), ERF3 (blue circles), and SBA-15 (black squares) as a function of the applied electric field measured by amplitude sweeps at constant strain, frequency and temperature of 0.01%, 10 rad s^{-1} and 20 °C, respectively. G' depends on the applied electric field and on the amount of MEPE or MC intercalated in SBA-15. Right (1) and (2): photos of ERF1 and ERF3 showing the characteristic dark blue and purple color of the composite in silicone oil, (3) photo of the pure white SBA-15 reference.

increases by about a factor of 4 from 3 to 12 kPa. The electrorheological effect of neat SBA-15 results from residual water, which was determined to be <1 wt % by thermoanalysis. Notably, for **ERF1** the modulus G′ increases by about a factor of 37 from 3 to 112 kPa and for **ERF2** by a factor of 53 from 3 to 158 kPa (Figure 2). Composites of mesoporous materials and charged polymers,[15−19] e.g., SBA-15 or MCM41 filled with polyaniline, pdot or organic salts, show similar or slightly higher effects as **ERF1** at medium field strengths but with five times higher concentrations ($\geq$0.5 wt %) of electroactive material in the dispersion. Although the concentration of MC as active material in **ERF3** is three times higher than the concentration of MEPE in **ERF1** the absolute ER-effect at 5 kV mm^{-1} is with 39 kPa three times lower. By further increasing the weight concentration of the MEPE/SBA-15 composite to 14.5 wt %, the storage modulus at 5 kV mm^{-1} yields 250 kPa. This value is a factor of 4 higher than comparable host−guest systems reported in the literature. Shear viscosity measurements using different concentrations (5, 10, and 14.5 wt %) of **ERF2** reveal that at least a concentration of 14.5 wt % is needed that the structure sustains at shear rates above 1 s^{-1} (see Figures S4 and S1 in the Supporting Information).

Although neat MEPE also shows a high electrorheological effect, the high current density renders neat MEPE unsuitable for practical applications. The presence of free charge carriers such as embedded water, acetic acid, acetate anions and MEPE chains themselves can contribute to the current. The current density increases with the applied potential; therefore, electric fields above 1 kV mm^{-1} are not realizable for the neat material. In contrast, in the composite, the charges are tightly confined to the host material and immobilized to the pore walls. The silica matrix itself is nonconducting. As a result, we measure values below 0.1 μA cm^{-2} for all ERF samples even at 5 kV mm^{-1}.

In the absence of an electric field, the charges of the MEPEs, the pore walls and the counterions are in equilibrium resulting in a neutral state of the composite. For the underlying mechanism of the ER-effect our hypothesis is that the external field will redistribute the charges in the pores. From the TEM analysis we know that the mesopores of SBA-15 have a preferential orientation along the particle long axis. On the basis of steric arguments, we assume that the MEPEs are oriented along this axis, whereas the MCs are randomly distributed in the pores. Therefore, a dipole moment may develop under the influence of an electric field along the pore axis.

Overall, the superposition of pore and MEPE orientation can maximize the individual contributions giving rise to a strong overall ER-effect even at low concentration of electro-active material. The resulting attractive interactions between dispersed particles results in the structure formation and the solidification of the fluid. While the exact mechanism is yet not fully understood, preliminary permittivity, $\varepsilon^* = \varepsilon' + i\varepsilon''$, measurements in the range of 0.01 Hz to 100 kHz reveal for **ERF1** a decreasing permittivity, ε', from 9 to 3, whereas for **REF**, ε' remains almost constant at approximately 2.8 (see Figure S5 in the Supporting Information). The higher ε' value of **ERF1** indicates the presence of a polarization mechanism in agreement with the ER-effect of **ERF1**. The dissipated energy is highest at the relaxation frequency, which corresponds to a maximum in the dielectric loss curve, ε'', at 2 Hz for **ERF1**. This value is below the generally accepted optimum range for ERFs between 0.1 and 100 kHz. The use of smaller particle is expected to increase the relaxation frequency to higher values.[20]

■ CONCLUSION

The application of electrorheological fluids is generally handicapped by high current densities, high basic viscosities or insufficient electrorheological activity. Here, we present an approach based on composites that has great potential to alleviate these deficiencies. Composites, made by intercalation of MEPEs in a single step into mesoporous SBA-15, dispersed in silicone oil show a strong electrorheological effect, even at very low concentration of active component with a negligible current density and a concomitant low basic viscosity. With G' > 110 kPa for 10 wt % of MEPE/SBA-15 composite dispersed in silicone oil corresponding to a concentration of 0.16 wt % of MEPE as active material, these composites outperform previously reported materials.[15−18] Due to the low current densities electric fields of more than 5 kV mm^{-1} can be applied. The advantages are the simple preparation, controlling MEPE loading by pH and solvent, the high stability, the excellent performance, and finally, the modular concept. We can choose different ligands, metal ions, counterions, and hosts (e.g., particle size, pore diameter) providing a multitude of options to tailor the electrorheological response of the resulting composites.

■ ASSOCIATED CONTENT

⑤ Supporting Information

Data of dielectric spectroscopy (ERF1 and REF), rotational rheology (ERF2), and amplitude sweeps (ERF1); SAXS curve of SBA-15; and photos of the fiberlike structure of ERF1 formed applying an electric field. This material is available free of charge via the Internet at http://pubs.acs.org.

■ AUTHOR INFORMATION

Corresponding Author
*E-mail: guntram.schwarz@matsyn.uni-wuerzburg.de.

Notes
The authors declare no competing financial interest.

■ ACKNOWLEDGMENTS

■ REFERENCES

(1) Halsey, T. C. *Science* **1992**, *258*, 761−766.

(2) Wen, W.; Huang, X.; Sheng, P. *Soft Matter* **2008**, *4*, 200−210.

(3) Wen, W.; Huang, X.; Yang, S.; Lu, K.; Sheng, P. *Nat. Mater.* **2003**, *2*, 727−730.

(4) Schwarz, G.; Sievers, T. K.; Bodenthin, Y.; Hasslauer, I.; Geue, T.; Koetz, J.; Kurth, D. G. *J. Mater. Chem.* **2010**, *20*, 4142−4148.

(5) Schütte, M.; Kurth, D. G.; Linford, M. R.; Cölfen, H.; Möhwald, H. *Angew. Chem., Int. Ed.* **1998**, *37*, 2891−2893.

(6) Schwarz, G.; Bodenthin, Y.; Tomkowicz, Z.; Haase, W.; Geue, T.; Kohlbrecher, J.; Pietsch, U.; Kurth, D. G. *J. Am. Chem. Soc.* **2011**, *133*, 547−558.

(7) Fulvio, P. F.; Pikus, S.; Jaroniec, M. *J. Colloid Interface Sci.* **2005**, *287*, 717−720.

(8) Akcakayiran, D.; Kurth, D. G.; Rohrs, S.; Rupprechter, G.; Findenegg, G. H. *Langmuir* **2005**, *21*, 7501−7506.

(9) Zhao, D.; Feng, J.; Huo, Q.; Melosh, N.; Fredrickson, G. H.; Chmelka, B. F.; Stucky, G. D. *Science* **1998**, *279*, 548−552.

(10) Winter, A.; Berg, A. M. J. v. d.; Hoogenboom, R.; Kickelbick, G.; Schubert, U. S. *Synthesis* **2006**, 2873−2878.

(11) Akcakayiran, D.; Mauder, D.; Hess, C.; K. Sievers, T.; Kurth, D. G.; Shenderovich, I.; Limbach, H.-H.; Findenegg, G. H. *J. Phys. Chem. B* **2008**, *112*, 14637−14647.

(12) Guo, Z.; Liu, X.-M.; Ma, L.; Li, J.; Zhang, H.; Gao, Y.-P.; Yuan, Y. *Colloids Surf., B* **2013**, *101*, 228−235.

(13) Salis, A.; Parsons, D. F.; Boström, M.; Medda, L.; Barse, B.; Ninham, B. W.; Monduzzi, M. *Langmuir* **2010**, *26*, 2484−2490.

(14) Neff, P. A.; Wunderlich, B. K.; v. Klitzing, R.; Bausch, A. R. *Langmuir* **2007**, *23*, 4048−4052.

(15) Liu, Y. D.; Fang, F. F.; Choi, H. J.; Seo, Y. *Colloids Surf., A* **2011**, *381*, 17−22.

(16) Fang, F. F.; Choi, H. J.; Ahn, W.-S. *Microporous Mesoporous Mater.* **2010**, *130*, 338−343.

(17) Cheng, Q.; Pavlinek, V.; He, Y.; Lengalova, A.; Li, C.; Saha, P. *Colloids Surf., A* **2008**, *318*, 169−174.

(18) Cho, M. S.; Choi, H. J.; Ahn, W.-S. *Langmuir* **2003**, *20*, 202−207.

(19) Cho, M. S.; Choi, H. J.; Kim, K. Y.; Ahn, W. S. *Macromol. Rapid Commun.* **2002**, *23*, 713−716.

(20) Sun, Y.; Thomas, M.; Masounave, J. *Smart Mater. Struct.* **2009**, *18*, 024004.